Matched-Pair Comparison of ^{68}Ga-PSMA-11 and ^{18}F-rhPSMA-7 PET/CT in Patients with Primary and Biochemical Recurrence of Prostate Cancer: Frequency of Non–Tumor-Related Uptake and Tumor Positivity

Markus Kroenke[1,2], Lilit Mirzoyan[2], Thomas Horn[3], Jan C. Peeken[4,5], Alexander Wurzer[6], Hans-Jürgen Wester[6], Marcus Makowski[1], Wolfgang A. Weber[2], Matthias Eiber[2], and Isabel Rauscher[2]

[1]Institute of Diagnostic and Interventional Radiology, School of Medicine, Technical University of Munich, Munich, Germany; [2]Department of Nuclear Medicine, School of Medicine, Technical University of Munich, Munich, Germany; [3]Department of Urology, School of Medicine, Technical University of Munich, Munich, Germany; [4]Department of Radiation Oncology, School of Medicine, Technical University of Munich, Munich, Germany; [5]Institute of Radiation Medicine, Department of Radiation Sciences, Helmholtz Zentrum München, Neuherberg, Germany; and [6]Pharmaceutical Radiochemistry, School of Medicine, Technical University of Munich. Munich, Germany

Radiohybrid prostate-specific membrane antigen (rhPSMA) ligands are a new class of prostate cancer theranostic agents. ^{18}F-rhPSMA-7 offers the advantages of ^{18}F labeling and low urinary excretion compared with ^{68}Ga-PSMA-11. Here, we compare the frequency of non–tumor-related uptake and tumor positivity with ^{68}Ga-PSMA-11 and ^{18}F-rhPSMA-7 in patients with primary or recurrent prostate cancer. **Methods:** This retrospective matched-pair comparison matched 160 ^{18}F-rhPSMA-7 with 160 ^{68}Ga-PSMA-11 PET/CT studies for primary staging (n = 33) and biochemical recurrence (n = 127) according to clinical characteristics. Two nuclear medicine physicians reviewed all scans, first identifying all PET-positive lesions and then differentiating lesions suggestive of prostate cancer from those that were benign, on the basis of known pitfalls and ancillary information from CT. For each region, the SUV_{max} of the lesion with the highest PSMA ligand uptake was noted. Tumor positivity rates were determined, and SUV_{max} was compared separately for each tracer. **Results:** ^{18}F-rhPSMA-7 and ^{68}Ga-PSMA-11 PET revealed 566 and 289 PSMA ligand–positive lesions, respectively. Of these, 379 and 100 lesions, equaling 67.0% and 34.6%, respectively, of all PSMA-positive lesions, were considered benign. The distribution of their etiology was similar (42%, 24%, and 25% with ^{18}F-rhPSMA-7 vs. 32%, 24%, and 38% with ^{68}Ga-PSMA-11 for ganglia, bone, and unspecific lymph nodes, respectively). All primary tumors were positive with both agents (n = 33 each), whereas slightly more metastatic lesions were observed with ^{68}Ga-PSMA-11 in both disease stages (113 for ^{18}F-rhPSMA-7 and 124 for ^{68}Ga-PSMA-11). The SUV_{max} of ^{18}F-rhPSMA-7 and ^{68}Ga-PSMA-11 did not differ ($P > 0.05$) in local recurrence or primary prostate cancer; however, the tumor-to-bladder ratio was significantly higher with ^{18}F-rhPSMA-7 (4.9 ± 5.3 vs. 2.2 ± 3.7, P = 0.02, for local recurrence; 9.8 ± 9.7 vs. 2.3 ± 2.6, $P < 0.001$, for primary prostate cancer). **Conclusion:** The tumor positivity rate was consistently high for ^{68}Ga-PSMA-11 and ^{18}F-rhPSMA-7. Both tracers revealed a considerable number of areas of uptake that were reliably identified as benign by trained physicians making use of corresponding morphologic imaging and known PSMA pitfalls. These were more frequent with ^{18}F-rhPSMA-7. However, the matched-pair comparison could have introduced a source of bias. Adequate reader training can allow physicians to differentiate benign uptake from disease and be able to benefit from the logistical and clinical advantages of ^{18}F-rhPSMA-7.

Key Words: PET; prostate cancer; prostate-specific membrane antigen (PSMA); radiohybrid PSMA (rhPSMA); 18F-rhPSMA-7; 68Ga-PSMA-11

J Nucl Med 2021; 62:1082–1088
DOI: 10.2967/jnumed.120.251447

Prostate-specific membrane antigen (PSMA) ligand PET is already recommended in various guidelines as the preferred imaging tool to localize disease in biochemical recurrence of prostate cancer (*1*,*2*). In the primary setting, a recently published prospective multicenter study on high-risk prostate cancer patients has confirmed the ability of ^{68}Ga-PSMA-11 PET/CT to accurately assess the site and extent of disease, providing superior accuracy in comparison to conventional imaging (*3*).

However, PSMA ligand PET may not be as specific for prostate cancer as initially thought, underlined by an increasing number of published case series describing increased PSMA ligand uptake in lesions attributed to a benign origin, such as ganglia, healing bone fracture, fibrous dysplasia, liver hemangioma, or non–prostate cancer malignancy (*4*,*5*).

Nowadays, ^{68}Ga-labeled PSMA ligands are increasingly replaced by ^{18}F-labeled compounds offering various advantages, including the lower positron energy of ^{18}F, potentially improving spatial resolution and reducing blurring effects; the longer half-life of ^{18}F; and high-yield production in cyclotrons. The latter two result in large-batch production suitable for long-distance distribution and potential cost savings. So far, various ^{18}F-labeled PSMA ligands (e.g., ^{18}F-PSMA-1007, ^{18}F-DCFPyL, and ^{18}F-rhPSMA-7) have been developed and show similarity to ^{68}Ga-PSMA-11 PET regarding detection rates in both primary staging and restaging

Received Jun. 11, 2020; revision accepted Nov. 12, 2020.
For correspondence or reprints, contact Isabel Rauscher (isabel.rauscher@tum.de).
Published online December 4, 2020.

(*6–9*). However, a recent matched-pair comparison in patients with recurrent prostate cancer described an approximately 5 times higher number of PSMA-positive lesions attributed to a benign origin (e.g., unspecific lymph nodes or ganglia) with ^{18}F-PSMA-1007 than with ^{68}Ga-PSMA-11, whereas similar cancer detection rates were observed (*10*). This finding raises questions about the frequency of non–prostate cancer PSMA-positive lesions with other ^{18}F-labeled PSMA ligands. Radiohybrid PSMA (rhPSMA) ligands are a new class of PSMA-targeting agents allowing fast and efficient ^{18}F labeling as well as the use of radiometals such as ^{68}Ga or ^{177}Lu (*11*). Because of rapid blood clearance but only minimal urinary excretion, potential advantages for local tumor assessment exist, as high tracer retention in the urinary tract and bladder is known to impair image interpretation.

Thus, the aim of this retrospective, matched-pair analysis was to compare differences in non–tumor-related PSMA ligand uptake and cancer detection efficacy between ^{18}F-rhPSMA-7 and ^{68}Ga-PSMA-11 PET/CT in patients with primary prostate cancer and those with biochemical recurrence.

MATERIALS AND METHODS

Patient Population

Data from 127 patients (median age, 72 ± 7 y; range, 52–84 y) with biochemical recurrence of prostate cancer after radical prostatectomy (median prostate-specific antigen [PSA] value, 0.70 ng/mL; range, 0.15–64.00 ng/mL) and 33 patients (median age, 71 ± 8 y; range, 52–83 y) with primary prostate cancer who underwent ^{18}F-rhPSMA-7 PET/CT at our institution between July 2017 and June 2018 were retrospectively included. Data from 127 corresponding patients (median age, 69 ± 8 y; range, 47–83 y) with biochemical recurrence of prostate cancer after radical prostatectomy (median PSA value, 0.65 ng/mL; range, 0.20–30.00 ng/mL) and 33 patients (median age, 69 ± 6 y; range, 56–75 y) with primary prostate cancer who had undergone ^{68}Ga-PSMA-11 PET/CT were identified in our institution's database, matched on the basis of various clinical parameters.

For the restaging cohort, the following clinical parameters were used: Gleason score (6–7 vs. 8–10), PSA value at time of PET (0.2–0.5, >0.5–1.0, >1.0–2.0, or >2 ng/mL), primary T-stage (≤2 vs. ≥3), primary N-stage (0 vs. 1), and use of androgen deprivation therapy within the 6 mo preceding examination (yes vs. no). Patients receiving salvage radiation therapy with regard to prostate cancer were excluded. The following criteria were used for the primary staging cohort: biopsy Gleason score (6–7 vs. 8–10) and PSA value at the time of PET (<10, >10–20, >20–30, or >30 ng/mL). None of the patients had received androgen deprivation therapy before. The characteristics of the matched-pair cohorts are summarized in Supplemental Table 1 (restaging cohort) and Supplemental Table 2 (primary staging cohort) (supplemental materials are available at http://jnm.snmjournals.org).

All patients gave written informed consent to anonymized evaluation and publication of their data. All reported investigations were conducted in accordance with the Helsinki Declaration and with national regulations. The retrospective analysis was approved by the Ethics Committee of the Technical University of Munich (permits 290/18S and 5665/13). The administration of ^{18}F-rhPSMA-7 and ^{68}Ga-PSMA-11 complied with the German Medicinal Products Act, paragraph13 2b, and with the requirements of the responsible regulatory body (Government of Oberbayern).

^{18}F-rhPSMA-7 and ^{68}Ga-PSMA-11 PET/CT

^{18}F-rhPSMA-7 was synthesized as recently reported by Wurzer et al. (*11*). ^{18}F-rhPSMA-7 (mean ± SD, 329 ± 48 MBq; range, 191–436 MBq) was administered as an intravenous bolus at 80 ± 20 min (range, 50–198 min) before the PET scan. ^{68}Ga-PSMA-11 was synthesized as reported by Eder et al. (*12*). ^{68}Ga-PSMA-11 was administered as an intravenous bolus (143 ± 31 MBq; range, 51–248 MBq), and the PET acquisition was started at 55 ± 9 min (range, 42–116 min) after tracer injection. All patients received 40 mg of furosemide and diluted oral contrast medium (mannitol, 25 mL/L). Contrast-enhanced PET/CT (Biograph mCT Flow; Siemens Medical Solutions) was performed as described previously (*13*,*14*). All PET scans were acquired in 3-dimensional mode with an acquisition time of 3–4 min per bed position or 1.1–1.5 mm/s using Biograph mCT Flow technique. Emission data were corrected for randoms, dead time, scatter, and attenuation and were reconstructed iteratively by ordered-subsets expectation maximization (4 iterations, 8 subsets) followed by a smoothing gaussian filter (5 mm in full width at half maximum), time-of-flight information, and resolution recovery (TrueX; Siemens). Matrix and image size were 200 × 200.

Image Analysis

All ^{68}Ga-PSMA-11 and ^{18}F-rhPSMA-7 PET/CT images (n = 320) were reviewed by 2 board-certified nuclear medicine physicians in consensus. First, all PSMA-positive lesions were noted and categorized as local, pelvic, abdomino- and supradiaphragmatic, bone, or other (e.g., lung or liver). In a second step, lesions suggestive of prostate cancer were differentiated from lesions that were most probably benign (e.g., ganglia, unspecific lymph nodes, fractures, or degenerative changes), taking into consideration the known pitfalls of PSMA PET imaging and information from contrast-enhanced CT. For each anatomic region, the SUV_{max} of the lesion with the highest PSMA ligand uptake was noted both for lesions suggestive of malignancy and for lesions attributed to a benign origin. To estimate the influence of high activity retention in the bladder, the SUV_{max} of the urinary bladder was measured and the tumor-to-bladder ratio for local tumors calculated. In addition, the shortest distance between a local recurrence and the bladder wall was measured in millimeters.

Statistical Analysis

Statistical analyses were performed using MedCalc software (version 13.2.0, 2014). All quantitative data are expressed as mean ± SD. P values of less than 0.05 were considered significant. Positivity rates for both primary and recurrent prostate cancer were determined, and the SUV_{max} of the most probably benign and the most suggestive lesions were compared separately for ^{68}Ga-PSMA-11 and ^{18}F-rhPSMA-7 PET/CT using a 2-sided t test.

RESULTS

Distribution and Localization of PSMA Ligand–Positive Lesions Attributed to Benign Origin

In total, ^{18}F-rhPSMA-7 and ^{68}Ga-PSMA-11 PET/CT revealed 566 and 289 lesions, respectively, with focal PSMA ligand uptake. Across both patient cohorts, ^{18}F-rhPSMA-7 PET revealed 379 lesions attributed to a benign origin, equaling 67.0% of all lesions, compared with 100 lesions equaling 34.6% for ^{68}Ga-PSMA-11 PET. In terms of absolute numbers, the number of lesions attributed to a benign origin was 3.8 higher for ^{18}F-rhPSMA-7 PET than for ^{68}Ga-PSMA-11 PET (4.8, 3.9, and 2.5 times more benign lesions in ganglia, bone, and unspecific lymph nodes, respectively) (Table 1, Fig. 1, and Supplemental Fig. 1).

The main site of PSMA ligand–positive lesions attributed to a benign origin were ganglia, bone lesions, and unspecific lymph nodes, with 32%, 24%, and 38%, respectively, of the positive non–prostate cancer findings in ^{68}Ga-PSMA-11 and 42%, 24%, and 25%, respectively, in ^{18}F-rhPSMA-7 PET. Most unspecific bone uptake was found in the ribs and in the spine; details on the exact distribution are presented in Supplemental Table 3. Uptake

TABLE 1
Regions Attributed to Benign Origin from All PSMA-Positive Regions

Origin	^{68}Ga-PSMA-11 PET		^{18}F-rhPSMA-7 PET	
	Benign regions	Benign regions/all regions	Benign regions	Benign regions/all regions
All lesions with benign origin	100	100/289 (34.6%)	379	379/566 (67.0%)
Unspecific lymph node				
Total	38/100 (38.0%)	38/132 (28.8%)	95/379 (24.8%)	95/171 (55.6%)
Pelvic		8/72		26/81
Abdomen + supradiaphragmatic		30/60		69/90
Ganglia				
Total	32/100 (32.0%)	32	159/379 (42.0%)	159
Cervical		13		62
Celiac		17		84
Sacral		2		13
Bone				
Total	24/100 (24.0%)	24/52 (46.2%)	94/379 (24.1%)	94/124 (75.8%)
Fracture		2		7
Degeneration		5		46
Unclear		3		5
Unspecific bone uptake		14		36
Other				
Total	6/100 (6.0%)	6/8 (87.5%)	31/379 (8.2%)	31/37 (83.7%)
Unspecific soft-tissue uptake*		6		29
Unclear uptake†		—		2

*Unspecific uptake (e.g., thyroid, skin, adenoma of adrenal gland, atelectasis with known PSMA ligand uptake) according to literature.
†Likely not tumor-related.
Data are number followed by percentage in parentheses.

in soft-tissue lesions attributed to a benign origin was seen rarely with both ^{68}Ga-PSMA-11 and ^{18}F-rhPSMA-7 PET (6% and 8%, respectively). Details on the absolute numbers and percentages of lesions rated as benign can be found in Table 1.

The SUV_{max} of lesions attributed to a benign origin was significantly higher ($P < 0.05$) with ^{18}F-rhPSMA-7 PET than with ^{68}Ga-PSMA-11 PET in ganglia (SUV_{max}, 5.2 ± 1.2 [range, 3.0–10.1] vs. 4.5 ± 1.0 [range, 3.2–7.0], respectively) and bone (SUV_{max}, 6.4 ± 3.5 [range, 3.2–24.2] vs. 5.0 ± 2.4 [range, 2.4–12.4], respectively) but not in unspecific lymph nodes (SUV_{max}, 4.9 ± 1.9 [range, 3.0–16.8] vs. 4.8 ± 1.2 [range, 3.5–9.6]). Examples of both ^{68}Ga-PSMA-11- and ^{18}F-rhPSMA-7 ligand uptake in benign lesions such as ganglia or axillary lymph nodes are presented in Figures 2 and 3. Supplemental Figure 2 demonstrates a histopathologically negative ^{18}F-rhPSMA-7–positive lesion in the ischial bone, and Supplemental Figure 3 visualizes 3 different ^{18}F-rhPSMA-7–positive bone lesions in the ribs: 1 rib metastasis, 1 fibroosseous lesion, and 1 area of unspecific uptake that was most probably benign.

Lesion Detection and Localization Attributed to Recurrent Prostate Cancer

In total, 187 ^{18}F-rhPSMA-7–positive lesions attributed to prostate cancer were found in 123 of the 160 patients, and 189 ^{68}Ga-PSMA-11–positive lesions attributed to prostate cancer were found in 124 of the 160 patients. The overall detection efficacy in patients with biochemical recurrence after radical prostatectomy, as a function of the PSA value, was identical for both ^{18}F-rhPSMA-7 and ^{68}Ga-PSMA-11 (56%, 77%, 64%, and 95% for PSA levels of <0.5, 0.5 to <1, 1 to <2, and >2 ng/mL, respectively). This matched-pair approach found a higher number of local recurrences with ^{18}F-rhPSMA-7 than with ^{68}Ga-PSMA-11 ($n = 42$ vs. $n = 32$) and a lower number of lymph node metastases ($n = 61$ vs. $n = 80$, respectively; Fig. 1C). A summary of lesions rated as malignant in patients with primary and biochemical recurrence of prostate cancer is presented (according to their origin) in Table 2.

Uptake and Tumor-to-Bladder Ratio of Local Recurrence and Primary Disease

All primary tumors were positive with ^{18}F-rhPSMA-7 and ^{68}Ga-PSMA-11 ($n = 33$ each), whereas a slightly higher number of metastatic lesions was observed with ^{68}Ga-PSMA-11 (113 with ^{18}F-rhPSMA-7 and 124 with ^{68}Ga-PSMA-11). The SUV_{max} in all local recurrences and primary tumors showed a trend to higher absolute values with ^{18}F-rhPSMA-7 than with ^{68}Ga-PSMA-11; however, the difference was not significant (19.3 ± 23.8 vs. 11.6 ± 10, $P = 0.06$, and 28.3 ± 22.6 vs. 18.9 ± 20.9, $P = 0.08$, respectively). The tumor-to-bladder ratio was significantly higher with ^{18}F-rhPSMA-7 than with ^{68}Ga-PSMA-11 in both local recurrence and primary tumor (4.9 ± 5.3 vs. 2.2 ± 3.7, $P = 0.02$, and 9.8

± 9.7 vs. 2.3 ± 2.6, $P < 0.001$, respectively). In ^{18}F-rhPSMA-7 and ^{68}Ga-PSMA-11 PET, local recurrence was directly adjacent to the urinary bladder in 19 of 42 patients (45.2%) and 19 of 32 patients (59.4%), respectively. In addition, local recurrent lesions identified by PSMA ligand imaging but not directly adjacent to the urinary bladder were a similar distance from the bladder wall on both ^{18}F-rhPSMA-7 PET and ^{68}Ga-PSMA-11 PET (mean, 8 ± 3 mm [range, 3–12 mm] and 8 ± 5 mm [range, 4–18 mm], respectively). A summary of lesions rated as malignant in patients with primary and biochemical recurrence of prostate cancer is presented (according to their origin) in Table 2.

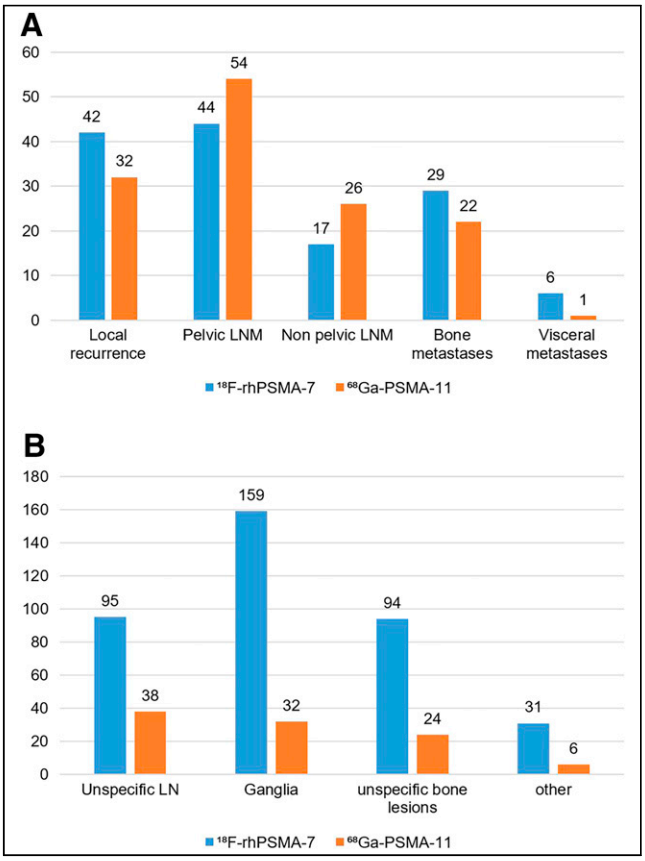

FIGURE 1. Localization of benign lesions (A) and localization of tumor lesions in patients with biochemical recurrence of prostate cancer after radical prostatectomy (B). LN = lymph nodes; LNM = lymph node metastases.

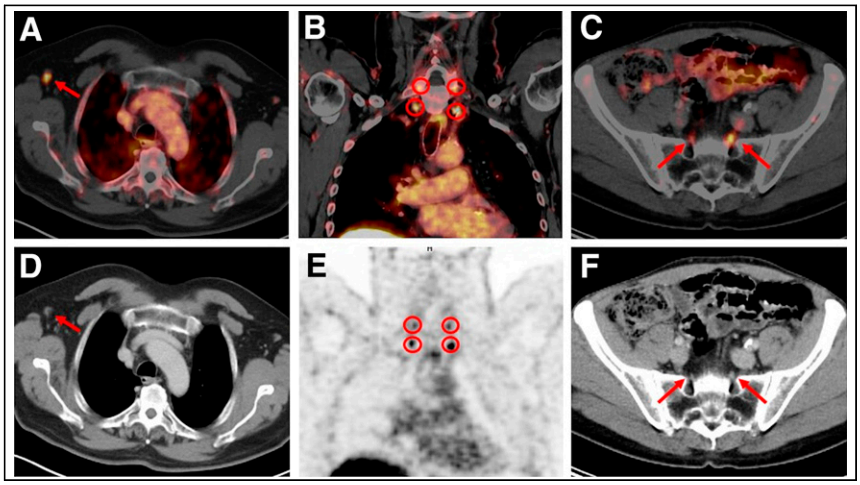

FIGURE 2. Examples of benign PSMA ligand uptake (arrows or encircled) on ^{18}F-rhPSMA-7 PET/CT (top) and CT (bottom, D and F) and PET (bottom, E). (A and D) Unspecific uptake in right axillary lymph node, with corresponding CT scan showing symmetric, nonenlarged lymph nodes with fat hilum sign. (B and E) Four ^{18}F-rhPSMA-7 ligand–positive cervical ganglia in typical location. (C and F) Two ^{18}F-rhPSMA-7 ligand–positive sacral ganglia.

DISCUSSION

Since the introduction of ^{68}Ga-PSMA-11 PET in 2011, there have been increasing reports of ^{68}Ga-PSMA-11 uptake in benign lesions such as ganglia and fractures (*15–18*). We conducted a matched-pair analysis in patients with primary and recurrent prostate cancer to explore uptake in benign lesions by ^{18}F-rhPSMA-7 compared with ^{68}Ga-PSMA-11 PET. Further, we evaluated the tumor positivity rates for ^{18}F-rhPSMA-7 and ^{68}Ga-PSMA-11, which were found to be similar. The 2 tracers identified sites of disease in a comparable way, with the limitation that a matched-pair approach is a potential source of bias. Taking into consideration the known pitfalls of PSMA imaging, along with the information from the corresponding contrast-enhanced CT scans, our experienced readers were able to disregard hot spots likely to be benign uptake. Such benign areas of uptake occurred more frequently with ^{18}F-rhPSMA-7 (66.8% of all ^{18}F-rhPSMA-7–positive lesions) than with ^{68}Ga-PSMA-11 (34.6% of all ^{68}Ga-PSMA-11–positive lesions). Our previous work including only patients with biochemical recurrence after radical prostatectomy showed that ^{18}F-PSMA-1007 also identified more benign lesions than ^{68}Ga-PSMA-11 PET when reported as a proportion of the total number of lesions identified by each tracer, respectively (66.4% vs. 29.2%) (*10*). As demonstrated by both these studies, areas of benign uptake are common with both ^{18}F- and ^{68}Ga-based PSMA ligands—although more frequent with ^{18}F-rhPSMA-7—and readers must be diligent in ruling these out as potential areas of malignancy, making use of resources such as corresponding CT scans.

In our analysis, the detection rate for recurrent prostate cancer was identical for both ^{68}Ga-PSMA-11 and ^{18}F-rhPSMA-7 ligands (both 70%) and was within the range of several other studies (*6*,*8*,*19*). Further, detection rates increased with PSA level in patients presenting with recurrent disease, from 56% at a PSA level of less than 0.5 ng/mL to 95% at a PSA level of more than 2 ng/mL. The comparable low detection rate (64%) in patients presenting with a PSA level of 1 to less than 2 ng/mL might be related to the low number of patients in this subgroup. A higher number of local recurrences was observed with ^{18}F-rhPSMA-7 than with ^{68}Ga-PSMA-11 (42 vs. 32 lesions; Fig. 1C) in our study, potentially because the lower excretion via the urinary tract in ^{18}F-rhPSMA-7 PET led to improved detection rates in regions directly adjacent to the urinary bladder, as was also described for ^{18}F-PSMA-1007 (*20*,*21*). Further, the tumor-to-background ratio in local recurrences was significantly higher with ^{18}F-rhPSMA-7 PET. ^{68}Ga-PSMA-11

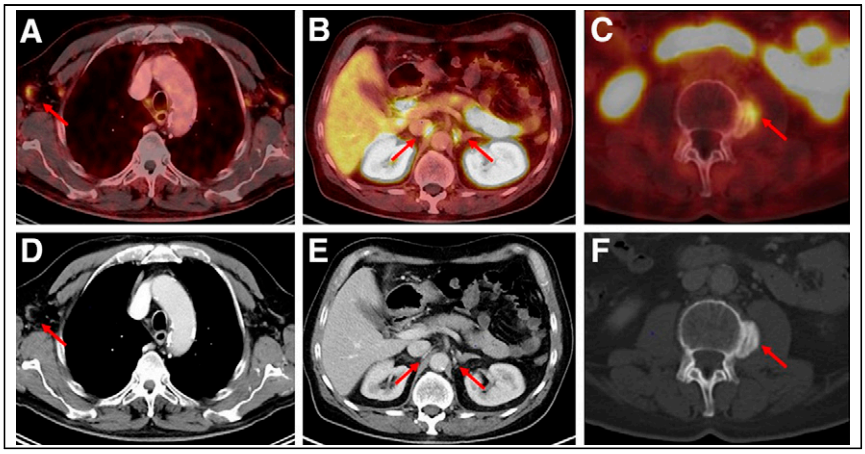

FIGURE 3. Examples of benign PSMA ligand uptake (arrows) on ^{68}Ga-PSMA-11 PET/CT (top) and CT (bottom). (A and D) Unspecific ^{68}Ga-PSMA-11 ligand uptake in right axillary lymph node, with corresponding CT scan showing oval, nonenlarged lymph nodes with fat hilum sign. (B and E) Two ^{68}Ga-PSMA-11 ligand–positive celiac ganglia in typical location. (C and F) ^{68}Ga-PSMA-11 ligand–positive osteophyte in lumbar spine.

identified a greater number of pelvic lymph node metastases than did ^{18}F-rhPSMA-7 (95 vs. 76, respectively, in both cohorts; Table 2). However, all results should be interpreted with caution, given the nature of this matched-pair comparison; despite matching based on clinical similarities, the different patient populations could have introduced bias and the different scanning routines could have an effect, especially on the SUV.

It is possible that the nature of the ^{18}F isotope contributes to the increased proportion of PSMA-positive benign lesions with ^{18}F-PSMA-7 PET than with ^{68}Ga-PSMA-11. This finding might be related the lower positron energy of ^{18}F than of ^{68}Ga, which improves spatial resolution, and to a higher signal from ^{18}F-PSMA-7 because it has a longer half-life and higher injected activities than ^{68}Ga-PSMA-11. Preclinical characteristics indicate that in PSMA-expressing cells or tumors, both ^{18}F-rhPMSA-7 and ^{18}F-PSMA-1007 have a higher affinity and internalization rate than does ^{68}Ga-PSMA-11, which could contribute to a higher signal from PSMA-expressing tissue (*11*,*18*). These results are in line with a recently published small histology-controlled dual PET/CT study in patients with intermediate- or high-risk prostate cancer (n = 16), by Kuten et al (*22*). In that study, both ^{68}Ga-PSMA-11 and PSMA-1007 PET ligands found all dominant lesions within the prostate whereas ^{18}F-PSMA-1007 PET revealed additional low-grade lesions, which often show lower PSMA expression.

The most common pitfalls in our study included uptake in ganglia (either cervical, celiac, or sacral), bone lesions, and unspecific lymph nodes (e.g., inguinal, axillary, or mediastinal), which occurred in 42%, 24%, and 25%, respectively, of patients with ^{18}F-rhPSMA-7 and in 32%, 24%, and 38%, respectively, of patients with ^{68}Ga-PSMA-11. This distribution is similar to that in previously published ^{18}F-PSMA-1007 PET patients matched to ^{68}Ga-PSMA-11 PET patients (43%, 24%, and 31%, respectively, with ^{18}F-PSMA-1007 and 29%, 27%, and 42%, respectively, with ^{68}Ga-PSMA-11) (*10*). Concordant with our results, Krohn et al. showed PSMA ligand uptake in celiac ganglia in 41% of patients (*23*). Along with the typical localization and shape of cervical, celiac, and sacral ganglia on CT images, this uptake should make differentiation from lymph node metastases easy for the well-trained reader. Two ongoing multicenter trials (NCT04186845 and NCT04186819) with ^{18}F-rhPSMA-7 will provide standardized reader training on such recognizable pitfalls and will test the performance of ^{18}F-rhPSMA-7 against a truth standard.

The reason for uptake of the PSMA ligands in histologically normal lymph nodes is not fully understood yet, although immunohistochemistry studies show that PSMA is expressed not only in cancerous tissues but also in intranodal vascular endothelia of lymph nodes (*24*). The difficulty with differentiating between unspecific and metastatic PSMA ligand uptake in lymph nodes for either tracer can be overcome with adequate training, and corresponding morphologic imaging can provide key information to delineate benign from malignant uptake (oval vs. round configuration, contrast enhancement, presence or absence of fat hilum sign), as can reading within the clinical context (pattern and extent of metastatic spread, PSA level).

TABLE 2
Location of Involved Regions Rated as Malignant in Both Staging and Restaging Cohorts

	^{68}Ga-PSMA-11 PET		^{18}F-rhPSMA-7 PET	
Location	Patients	Involved regions	Patients	Involved regions
Patients with suggestive lesions	124/160 (77.5%)	189	123/160 (76.9%)	187
Local	65/160 (40.6%)	65/189 (34.4%)	75/160 (46.9%)	75/187 (40.1%)
Lymph node metastases	78/160 (48.8%)	95/189 (50.3%)	61/160 (38.1%)	76/187 (41.1%)
Pelvic		65		55
Extrapelvic		30		21
Bone metastases	28/160 (17.5%)	28/189 (14.8%)	30/160 (18.8%)	30/187 (16.0%)
Other metastases	1/160 (0.6%)	1/189 (0.6%)	6/160 (3.8%)	6/187 (3.2%)

Data are number followed by percentage in parentheses.

Benign PSMA ligand–positive bone findings have been described before and accounted for 24% of all PSMA-positive lesions attributed to a benign origin in our study (*4*,*15*,*25*). Fracture lines, osteophytes, or fibroosseous lesions can easily be resolved with side-by-side evaluation of PET and CT images; however, the fact that there is a comparably high amount of PSMA ligand uptake in the bone (mainly ribs and spine) without a clear correlate on CT images remains a diagnostic challenge. On the basis of low to intermediate PSMA ligand uptake, and considering the patient history, many of these cases were classified as unspecific.

There were several limitations to our study. First, this was a retrospective matched-pair comparison. Therefore, the comparison of detection rates is inherently of lower validity than in a dual imaging protocol using both tracers. Although we aimed for similar clinical characteristics between the 2 cohorts, the different patient populations are a source of potential bias. However, the cohorts should be sufficient at least to compare benign or unspecific tracer uptake. Second, a rigorous validation of PSMA ligand–positive lesions by histopathology or immunohistopathology was not performed. However, a very high positive predictive value for PSMA ligand PET, considering the known limitations and pitfalls, has been shown in several studies (*26*). Because lesions attributed to a benign origin, such as ganglia or unspecific lymph nodes, are usually not validated histopathologically, corresponding contrast-enhanced CT images served as a reference. However, many institutions perform only low-dose CT in combination with the PET scan, potentially influencing the specificity of the scans; this potential would be even greater with ^{18}F-rhPSMA-7, given the higher amount of non–tumor-related PSMA ligand uptake. Therefore, especially before starting local therapies, we recommend the use of PSMA ligand PET with contrast-enhanced CT to avoid, for example, follow-up imaging and biopsies in order to clarify unclear findings, leading to increasing costs for the public health system.

Third, patients receiving ^{18}F-rhPSMA-7 were scanned later than those receiving ^{68}Ga-PSMA-11 (80 vs. 55 min after injection, respectively). Thus, direct comparisons of SUV_{max} in our study have to be handled with caution because several studies suggest that at later imaging time points, most lesions have a higher SUV (*27*,*28*). Further, the mean injected activity of ^{18}F-rhPSMA-7 was higher than that of ^{68}Ga-PSMA-11 (mean, 329 vs. 143 MBq, respectively) but was within the range of activities used in different prospective studies (e.g., CONDOR, OSPREY, LIGHTHOUSE, and SPOTLINE). However, a precise comparison of both tracers would need use of the same acquisition times and the same injected activities. A further limitation of this work was the use of a point-spread function recovery algorithm, which may exacerbate benign uptake of the ^{18}F isotope. Further prospective studies are necessary and warranted to overcome these limitations.

CONCLUSION

The tumor positivity rate was consistently high for each tracer. Both ^{68}Ga-PSMA-11 and ^{18}F-rhPSMA-7 revealed a considerable number of areas of uptake that were reliably identified as benign by trained physicians making use of corresponding contrast-enhanced CT imaging and known PSMA pitfalls. Notwithstanding the potential biases introduced by the case-matching methodology and different scanning routines, the frequency of these findings was clearly higher with ^{18}F-rhPSMA-7, in keeping with prior work on ^{18}F-PSMA-1007. Adequate reader training can allow physicians to differentiate benign uptake from disease and be able to benefit from the logistical advantages of ^{18}F-rhPSMA-7.

DISCLOSURE

A patent application has been submitted for rhPSMA (Hans-Jürgen Wester, Alexander Wurzer, and Matthias Eiber, inventors). Hans-Jürgen Wester and Matthias Eiber received funding from the SFB 824 (DFG Sonderforschungsbereich 824, project B11) from the Deutsche Forschungsgemeinschaft (Bonn, Germany) and Blue Earth Diagnostics Ltd. (Oxford, U.K., licensee for rhPSMA) as part of an academic collaboration. Matthias Eiber and Wolfgang Weber are consultants for Blue Earth Diagnostics Ltd. Hans-Jürgen Wester is founder, shareholder, and advisory board member of Scintomics GmbH (Fuerstenfeldbruck, Germany). Siemens Medical Solutions (Erlangen, Germany) supported the application of Biograph mCT Flow as part of an academic collaboration. No other potential conflict of interest relevant to this article was reported.

KEY POINTS

QUESTION: Is the frequency of non–tumor-related PSMA ligand uptake and detection efficacy comparable in matched-pair cohorts of ^{68}Ga-PSMA-11 and ^{18}F-rhPSMA-7 PET/CT patients with both primary and recurrent prostate cancer?

PERTINENT FINDINGS: Both ^{68}Ga-PSMA-11 and ^{18}F-rhPSMA-7 revealed areas of benign uptake. The proportion was clearly greater with ^{18}F-rhPSMA-7 but can be overcome with adequate reader training. The tumor positivity rates were similar for both radiopharmaceuticals.

IMPLICATIONS FOR PATIENT CARE: After adequate training, physicians should be able to reliably identify pitfalls, fully exploiting the logistical advantages of ^{18}F-rhPSMA-7 and its low urinary excretion.

REFERENCES

1. Perera M, Papa N, Christidis D, et al. Sensitivity, specificity, and predictors of positive ^{68}Ga-prostate-specific membrane antigen positron emission tomography in advanced prostate cancer: a systematic review and meta-analysis. *Eur Urol.* 2016;70:926–937.
2. Cornford P, Bellmunt J, Bolla M, et al. EAU-ESTRO-SIOG guidelines on prostate cancer. Part II: treatment of relapsing, metastatic, and castration-resistant prostate cancer. *Eur Urol.* 2017;71:630–642.
3. Hofman MS, Lawrentschuk N, Francis RJ, et al. Prostate-specific membrane antigen PET-CT in patients with high-risk prostate cancer before curative-intent surgery or radiotherapy (proPSMA): a prospective, randomised, multicentre study. *Lancet.* 2020;395:1208–1216.
4. Hofman MS, Hicks RJ, Maurer T, Eiber M. Prostate-specific membrane antigen PET: clinical utility in prostate cancer, normal patterns, pearls, and pitfalls. *Radiographics.* 2018;38:200–217.
5. Sheikhbahaei S, Werner RA, Solnes LB, et al. Prostate-specific membrane antigen (PSMA)-targeted PET imaging of prostate cancer: an update on important pitfalls. *Semin Nucl Med.* 2019;49:255–270.
6. Giesel FL, Knorr K, Spohn F, et al. Detection efficacy of ^{18}F-PSMA-1007 PET/CT in 251 patients with biochemical recurrence of prostate cancer after radical prostatectomy. *J Nucl Med.* 2019;60:362–368.
7. Mena E, Lindenberg ML, Turkbey IB, et al. ^{18}F-DCFPyL PET/CT imaging in patients with biochemically recurrent prostate cancer after primary local therapy. *J Nucl Med.* 2020;61:881–889.
8. Eiber M, Kroenke M, Wurzer A, et al. ^{18}F-rhPSMA-7 PET for the detection of biochemical recurrence of prostate cancer after radical prostatectomy. *J Nucl Med.* 2020;61:696–701.

9. Kroenke M, Wurzer A, Schwamborn K, et al. Histologically confirmed diagnostic efficacy of ^{18}F-rhPSMA-7 PET for N-staging of patients with primary high-risk prostate cancer. *J Nucl Med.* 2020;61:710–715.
10. Rauscher I, Kronke M, Konig M, et al. Matched-pair comparison of ^{68}Ga-PSMA-11 PET/CT and ^{18}F-PSMA-1007 PET/CT: frequency of pitfalls and detection efficacy in biochemical recurrence after radical prostatectomy. *J Nucl Med.* 2020;61:51–57.
11. Wurzer A, Di Carlo D, Schmidt A, et al. Radiohybrid ligands: a novel tracer concept exemplified by ^{18}F- or ^{68}Ga-labeled rhPSMA inhibitors. *J Nucl Med.* 2020;61:735–742.
12. Eder M, Neels O, Muller M, et al. Novel preclinical and radiopharmaceutical aspects of [^{68}Ga]Ga-PSMA-HBED-CC: a new PET tracer for imaging of prostate cancer. *Pharmaceuticals (Basel).* 2014;7:779–796.
13. Souvatzoglou M, Eiber M, Martinez-Moeller A, et al. PET/MR in prostate cancer: technical aspects and potential diagnostic value. *Eur J Nucl Med Mol Imaging.* 2013;40(suppl 1):S79–S88.
14. Eiber M, Maurer T, Souvatzoglou M, et al. Evaluation of hybrid ^{68}Ga-PSMA ligand PET/CT in 248 patients with biochemical recurrence after radical prostatectomy. *J Nucl Med.* 2015;56:668–674.
15. Sheikhbahaei S, Afshar-Oromieh A, Eiber M, et al. Pearls and pitfalls in clinical interpretation of prostate-specific membrane antigen (PSMA)-targeted PET imaging. *Eur J Nucl Med Mol Imaging.* 2017;44:2117–2136.
16. Keidar Z, Gill R, Goshen E, et al. ^{68}Ga-PSMA PET/CT in prostate cancer patients: patterns of disease, benign findings and pitfalls. *Cancer Imaging.* 2018;18:39.
17. Shetty D, Patel D, Le K, Bui C, Mansberg R. Pitfalls in gallium-68 PSMA PET/CT interpretation: a pictorial review. *Tomography.* 2018;4:182–193.
18. Eder M, Schafer M, Bauder-Wust U, et al. ^{68}Ga-complex lipophilicity and the targeting property of a urea-based PSMA inhibitor for PET imaging. *Bioconjug Chem.* 2012;23:688–697.
19. Perera M, Papa N, Roberts M, et al. Gallium-68 prostate-specific membrane antigen positron emission tomography in advanced prostate cancer: updated diagnostic utility, sensitivity, specificity, and distribution of prostate-specific membrane antigen-avid lesions—a systematic review and meta-analysis. *Eur Urol.* 2020;77:403–417.
20. Rahbar K, Weckesser M, Ahmadzadehfar H, et al. Advantage of ^{18}F-PSMA-1007 over ^{68}Ga-PSMA-11 PET imaging for differentiation of local recurrence vs. urinary tracer excretion. *Eur J Nucl Med Mol Imaging.* 2018;45:1076–1077.
21. Rahbar K, Afshar-Oromieh A, Seifert R, et al. Diagnostic performance of ^{18}F-PSMA-1007 PET/CT in patients with biochemical recurrent prostate cancer. *Eur J Nucl Med Mol Imaging.* 2018;45:2055–2061.
22. Kuten J, Fahoum I, Savin Z, et al. Head-to-head comparison of ^{68}Ga-PSMA-11 with ^{18}F-PSMA-1007 PET/CT in staging prostate cancer using histopathology and immunohistochemical analysis as a reference standard. *J Nucl Med.* 2020;61:527–532.
23. Krohn T, Verburg FA, Pufe T, et al. [^{68}Ga]PSMA-HBED uptake mimicking lymph node metastasis in coeliac ganglia: an important pitfall in clinical practice. *Eur J Nucl Med Mol Imaging.* 2015;42:210–214.
24. Afshar-Oromieh A, Sattler LP, Steiger K, et al. Tracer uptake in mediastinal and paraaortal thoracic lymph nodes as a potential pitfall in image interpretation of PSMA ligand PET/CT. *Eur J Nucl Med Mol Imaging.* 2018;45:1179–1187.
25. Jochumsen MR, Dias AH, Bouchelouche K. Benign traumatic rib fracture: a potential pitfall on ^{68}Ga-prostate-specific membrane antigen PET/CT for prostate cancer. *Clin Nucl Med.* 2018;43:38–40.
26. Rauscher I, Maurer T, Beer AJ, et al. Value of ^{68}Ga-PSMA HBED-CC PET for the assessment of lymph node metastases in prostate cancer patients with biochemical recurrence: comparison with histopathology after salvage lymphadenectomy. *J Nucl Med.* 2016;57:1713–1719.
27. Afshar-Oromieh A, Sattler LP, Mier W, et al. The clinical impact of additional late PET/CT imaging with ^{68}Ga-PSMA-11 (HBED-CC) in the diagnosis of prostate cancer. *J Nucl Med.* 2017;58:750–755.
28. Afshar-Oromieh A, Hetzheim H, Kubler W, et al. Radiation dosimetry of ^{68}Ga-PSMA-11 (HBED-CC) and preliminary evaluation of optimal imaging timing. *Eur J Nucl Med Mol Imaging.* 2016;43:1611–1620.